Observation of Level Crossing in H, $n=2$*†

R. T. Robiscoe‡

Ryerson Laboratory, Department of Physics, University of Chicago, Chicago, Illinois

(Received 27 July 1964; revised manuscript received 30 November 1964)

We have observed the crossing of the atomic hydrogen levels $\beta_B(2S_{1/2}, m_J=-\frac{1}{2}, m_I=-\frac{1}{2})$ and $e_B(2P_{1/2}, m_J=+\frac{1}{2}, m_I=-\frac{1}{2})$ near 605 G. A new atomic-beam method is used. H atoms are excited to the metastable $2S$ state by electron bombardment. The $2S(m_J=-\frac{1}{2})$ state is quenched in the bombardment region. The $2S(m_J=+\frac{1}{2})$ beam passes through a zero-field region where $\frac{1}{3}$ of it is converted to the single hyperfine level β_B. The β_B atoms enter a uniform magnetic field parallel to the beam. With no externally applied electric field, 92% of them reach the detector. When we apply an electrostatic field of about 0.7 V/cm perpendicular to the beam, the β_B atoms are strongly quenched near the β_B-e_B crossing point. Observed quenching agrees with the Bethe-Lamb theory of the $2S$ lifetime in external fields. We measure magnetic field by the nuclear magnetic resonance frequency of protons in water. Natural asymmetry and minor experimental corrections reduce the observed center of the β_B-e_B quenching resonance by 1 part in 10^4. The corrected β_B-e_B crossing occurs at 2577.57±0.25 kc/sec, proton nmr in water. From this, we calculate the Lamb shift S in H, $n=2$. With a diamagnetic shielding correction, and the accurately known $2S$ hyperfine interval, we get $S=1058.07$ ±0.10 Mc/sec. This disagrees with $S=1057.77$±0.10 Mc/sec from the Lamb experiments.

I. INTRODUCTION AND EXPERIMENTAL METHOD

THE beautiful experiments of Lamb and co-workers[1] established an atomic-beam, radio-frequency method which gave precise measurements of the fine structure (fs) in the $n=2$ level of atomic hydrogen. This fs is shown in Fig. 1. By combining careful measurements of the intervals $2S_{1/2}-2P_{1/2}$ (the so-called Lamb shift) and $2P_{3/2}-2S_{1/2}$, Lamb obtained the $2P_{3/2}-2P_{1/2}$ separation at zero field to an accuracy of 18 ppm.[2] This measurement provides one of the most accurate values for the fs constant α.[3]

A remeasurement of α has been suggested by Greenberg and Foley.[4] They point out that an increase in α by ≈ 15 ppm would explain the present discrepancy between measurement and calculation of the hyperfine structure (hfs) in the ground state of atomic hydrogen. A remeasurement of α producing a more accurate value would facilitate comparison between recent experiments[5-8] and quantum electrodynamical calculations, which depend upon α as the fundamental expansion parameter. Several experiments are in progress to remeasure α. It is hoped that a measurement of the fs in the 2^3P state of He,[9] together with a calculation of the He fs intervals,[10] will give α accurate to 1 ppm. Measurement of the hfs in the ground state of muonium has recently confirmed Lamb's value for α.[11]

A remeasurement of the fs in H, $n=2$, also provides a redetermination of α. The present paper describes a new method which can be used to remeasure this fs, by locating the crossing points between $2S$ and $2P$ levels in the Zeeman diagram of Fig. 1. We have used this method to measure the first crossing point in H, occur-

[1] The articles on the fine structure of atomic hydrogen are referred to as HI to HVI. They are: HI, W. E. Lamb, Jr., and R. C. Retherford, Phys. Rev. 79, 549 (1950); HII, W. E. Lamb, Jr., and R. C. Retherford, ibid. 81, 222 (1951); HIII, W. E. Lamb, Jr., ibid. 85, 259 (1952); HIV, W. E. Lamb, Jr., and R. C. Retherford, ibid. 86, 1014 (1952); HV, S. Triebwasser, E. S. Dayhoff, and W. E. Lamb, Jr., ibid. 89, 98 (1953); HVI, E. S. Dayhoff, S. Triebwasser, and W. E. Lamb, Jr., ibid. 89, 106 (1953).

[2] See HV and HVI, Ref. 1.

[3] See Sec. 109 in HVI, Ref. 1, for calculation of α from the $2P_{3/2}-2P_{1/2}$ interval. The value of α derived by Lamb was changed by correction of the fourth-order anomalous electron moment calculation. The corrected value is $\alpha=1/(137.0390$ ±0.0012). See discussion in H. Bethe and E. Salpeter Quantum Mechanics of One and Two-Electron Atoms (Academic Press Inc., New York, New York, 1957), 1st ed., p. 352. This text will be referred to later as BS(57).

[4] D. A. Greenberg and H. M. Foley, Phys. Rev. 120, 1684 (1960).

[5] The measurement of the Lamb shift in H and D (S. Triebwasser, E. S. Dayhoff, and W. E. Lamb, Jr., HV, Ref. 1) and in He⁺ [E. Lipworth and R. Novick, Phys. Rev. 108, 1434 (1957)] can be compared with calculations to relative order $(Z\alpha)^2\ln(Z\alpha)$ [A. J. Layzer, J. Math. Phys. 2, 308 (1961)].

[6] Measurement of the free-electron g value [D. T. Wilkinson and H. R. Crane, Phys. Rev. 130, 852 (1963)] can be compared with calculations to relative order α^2 [C. M. Sommerfield, Ann. Phys. (N.Y.) 5, 26 (1958)].

[7] Measurement of the ratio of the $2S$ to $1S$ hfs in H and D [J. Heberle, H. Reich, and P. Kusch, Phys. Rev. 101, 612 (1956); 104, 1585 (1956)] can be compared with calculations to relative order α^3 [D. E. Zwanziger, Phys. Rev. 121, 1128 (1961)] and $\alpha^2(m/M)$ [M. M. Sternheim, ibid. 130, 211 (1963)].

[8] The accurately measured hfs in the ground state of H [S. Crampton, D. Kleppner, and N. Ramsey, Phys. Rev. Letters 11, 338 (1963)] can be compared with calculations to relative order $\alpha^3\ln\alpha$ [D. E. Zwanziger, Bull. Am. Phys. Soc. 6, 514 (1961); A. J. Layzer, ibid. 6, 514 (1961)]. Measurement is higher than theory by about 43±21 ppm, with the uncertainty mainly due to inaccuracy in α. The discrepancy is probably due to inadequate evaluation of proton structure corrections. See Ref. 11.

[9] F. D. Colegrove, P. A. Franken, R. R. Lewis, and R. H. Sands, Phys. Rev. Letters 3, 420 (1959). See also F. Pichanick, R. Swift, and V. Hughes, Bull. Am. Phys. Soc. 9, 90 (1964). Pichanick quotes an accuracy of ±3 ppm in the measurement of the $J=2$ to $J=1$ fs interval in 2^3P of He (private communication).

[10] C. M. Schwartz, Phys. Rev. 134, A1181 (1964).

[11] The value $\alpha^{-1}=137.0388$±0.0012 has been reported as the result of measurement of the ground-state hfs interval in muonium by W. Cleland, J. Bailey, M. Eckhause, V. Hughes et al., Phys. Rev. Letters 13, 202 (1964). The agreement with Lamb's result strongly indicates that the hydrogen hfs discrepancy is due to incorrect proton structure corrections.

ring between levels $\beta(2S_{1/2}, m_J = -\frac{1}{2})$ and $e(2P_{1/2}, m_J = +\frac{1}{2})$, near 575 G. This measurement yields a value for the Lamb shift. In principle, our method could be used to measure the crossing between levels $\alpha(2S_{1/2}, m_J = +\frac{1}{2})$ and $c(2P_{3/2}, m_J = -\frac{1}{2})$. This would give the $2P_{3/2}-2S_{1/2}$ interval, which—together with the Lamb shift measurement—would determine the total fs.

Our crossing-point method for measuring the Lamb shift in H, $n=2$, differs from Lamb's rf method in several respects. Instead of using radio frequency to induce $2S-2P$ transitions, we use a static electric field. By producing a beam of β's in the pure state $\beta_B(2S_{1/2}, m_J = -\frac{1}{2}, m_I = -\frac{1}{2})$, we eliminate complications due to hfs. This, together with a Zeeman magnetic field parallel to the beam trajectory, reduces experimental corrections and sources of systematic error.

The remainder of this section compares our method with Lamb's, and qualitatively describes our experiment. Sections II and III give details of our apparatus, procedure and results. Section IV is a calculation of the Lamb shift from our observation of the β-e crossing point. In Sec. V, we compare our results with Lamb's and with theory.

A. Comparison of Lamb Method and Crossing Point Method

The Lamb method exploits the metastability of the $2S$ state. A beam of H atoms, made by the thermal dissociation of H_2, is excited to the $2S$ state by electron bombardment. In the absence of external fields, the $2S$ atoms live long enough ($\approx \frac{1}{8}$ sec) to be detected by electron ejection upon impact at a metal surface. In the Lamb experiments, the $2S$ atoms are subjected in midflight to a rf signal which induces a transition to a short-lived $2P$ state (lifetime $\approx 1.6 \times 10^{-9}$ sec). The $2S$ atoms are thereby quenched (by decay to ground state via emission of Lyman-α radiation) and do not reach the detector. At fixed radio frequency, a scan of magnetic field produces a $2S$ quenching curve with a resonance at that magnetic field H_c where the $2S-2P$ separation is equal to the applied radio frequency.

Since each fs level in Fig. 1 has two hfs levels associated with it, this curve is complicated by hfs. Two resonances actually occur, one for each of the $2S-2P$ transitions with $\Delta m_I = 0$. Thus, the $2S$ quenching resonance is the superposition of two hfs resonances, slightly above and below H_c. The center of this composite resonance, corrected for hfs and Zeeman curvature, gives the $2S-2P$ fs separation corresponding to H_c. Extrapolation to zero field gives the fs interval for the $2S-2P$ states involved. Using α-e and α-f transitions, Lamb and co-workers measured the $2S_{1/2}-2P_{1/2}$ fs interval S (the Lamb shift) in hydrogen to an accuracy of 100 ppm.[12]

Our method for measuring S is simpler. Instead of using radio frequency to induce transitions between the
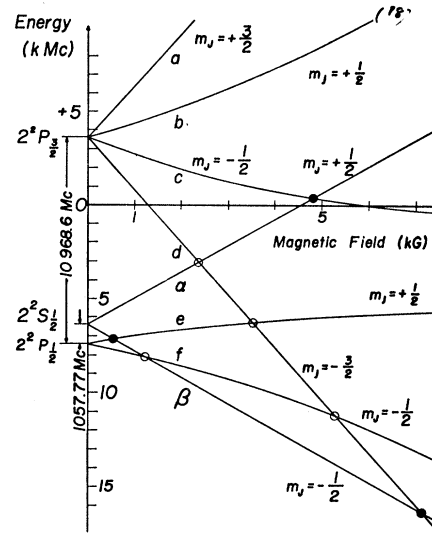
[12] HV, See Ref. 1, Sec. 94. Result is $S = 1057.77 \pm 0.10$ Mc/sec.

FIG. 1. Zeeman diagram of the fine structure in H, $n=2$. The levels $a, \cdots, \beta$ are Lamb's designation. The present experiment is concerned with the measurement of the crossing point between levels β and e, near 575 G. The α-c and β-d crossing points could be measured by the present technique.

$2S$ state α and $2P$ states, we use a static electric field to induce a transition between the $2S$ state β and the $2P$ state e. Figure 2 shows the magnetic field dependence of states β and e and includes hfs. At a small fixed electrostatic field ≈ 1 V/cm, a scan of magnetic field in the vicinity of the β-e crossing near 575 G produces a $2S$ quenching curve with a resonance at the β-e crossing-point field. In our early work,[13] we observed a $2S$ quenching resonance with resolvable peaks at the hfs crossings A and B (transitions with $\Delta m_I = 0$) indicated
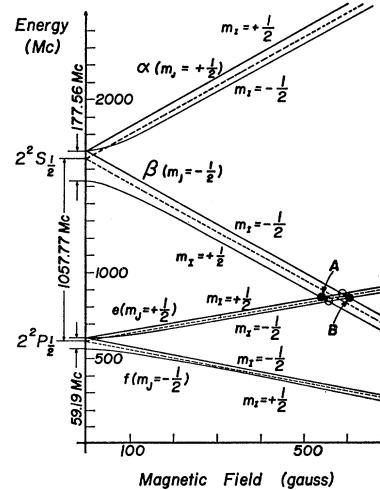

FIG. 2. Zeeman diagram of the $J = \frac{1}{2}$ levels in H, $n=2$, including hyperfine structure (hfs). The β-e crossing consists of four hfs crossings. Crossings A and B, with $\Delta m_I = 0$, have been observed. Crossing point B has been isolated and measured.

[13] W. L. Lichten and R. T. Robiscoe, Bull. Am. Phys. Soc. 8, 429 (1963).

in Fig. 2. Later, we isolated the peak at B and used it to measure the β-e crossing. This elimination of the hfs complication considerably reduces the resonance line-width, and simplifies the analysis of the quenching line shape.

B. Elimination of the hfs Complication

In order to eliminate the hfs complication, the crossing-point experiment is performed using a $2S$ beam containing only *one* hfs component $\beta_B(m_I=-\frac{1}{2})$ of the state β. This beam is produced in the following way. We place the electron gun (electron bombardment region) in a 575 G field perpendicular to the beam. This brings the β's to the β-e crossing point. As soon as β's are produced, they are strongly quenched by a motional electric field ≈ 3.5 V/cm owing to passage through the perpendicular 575 G field. Additional β quenching occurs (by β-f mixing) by electric fields ~ 10 V/cm associated with the electron bombardment current. The residual $2S$ beam is polarized in the state α. Measurements show this beam does not contain more than 1 part in 20 000 of the β component. After leaving the electron gun, the α beam passes through a region where the magnetic field is brought to zero and may even be adjusted to a small negative value. Here the α's lose their axis of quantization and a redistribution of states occurs (Majorana flop). One-third of the α beam enters the β_B state, which is degenerate with α at zero magnetic field. The state $\beta_A(m_I=+\frac{1}{2})$ is not regenerated because it is well separated (by ≈ 177 Mc/sec) from α at zero field. The beam is now two-thirds α, and one-third β_B. Therefore, as we perform the crossing-point experiment, we observe only the quenching peak at crossing-point B, between levels $\beta_B(2S_{1/2},\ m_J=-\frac{1}{2},\ m_I=-\frac{1}{2})$ and $e_B(2P_{1/2},\ m_J=+\frac{1}{2},\ m_I=-\frac{1}{2})$.
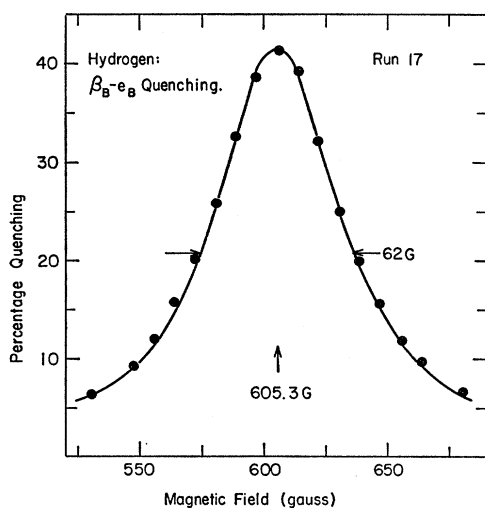

FIG. 4. Apparatus schematic: S, collimating slit; F, flopper; C_1 and C_2, collimating caps; E, electrostatic shield; Q, quenching region; P, proton nmr probe.

The β_B-e_B peak is symmetric about the crossing-point field $H_{CB}\approx 605$ G. Figure 3 shows an experimental line shape. No trace of a residual contribution from crossing-point A is observed. The experimental points are compared with a line shape derived from the Bethe-Lamb theory[14] for the life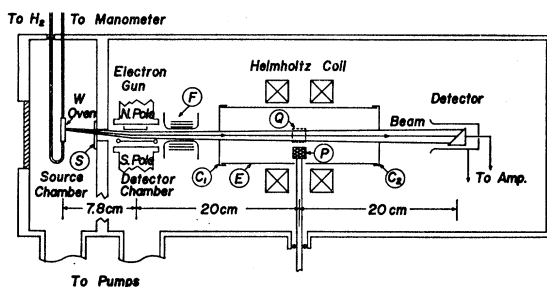time of the $2S$ state in external fields. Several effects which make the line slightly asymmetric about H_{CB}, mainly owing to natural causes such as the Zeeman curvature of the level e_B, are too small to be seen on the scale of Fig. 3. These effects cause the observed line center H_{CB}' to lie above the true center H_{CB} by about 1 part in 10^4.

Because the line asymmetry corrections are small, and because the theory of such a quenching resonance is given by Lamb, pertinent theoretical remarks are committed to Appendices. Appendix I treats the line itself. Appendix II gives the asymmetry corrections we have used. Section IV deals with the calculation of S from a total of 124 measurements of the β_B-e_B line center.

II. EXPERIMENTAL APPARATUS

A. Production and Detection of the Metastable Beam

Figure 4 is an apparatus schematic. The source of atoms is a tungsten oven,[15] modeled after Hendrie's improvement of Lamb and Retherford's original design.[16] A current of 250A ac heats the oven to 3000°K, as measured with a pyrometer.[17] Molecular hydrogen is admitted until the oven pressure is about 1 mm. Under these conditions, we measure $\approx 96\%$ dissociation. In the final runs, the atomic beam was stable to 5 parts in 10^4.

FIG. 3. Observation of quenching of the metastable state β_B near the β_B-e_B crossing point. The experimental points are compared with a line shape derived from the Bethe-Lamb theory of the lifetime of the $2S$ state in external fields.

---

[14] See HI, Ref. 1, Appendix II. Also see discussion in Sec. 67 of BS(57), Ref. 3.

[15] The oven is made of tungsten tubing, available from Wheaton Industries, Addison, Illinois. A 0.200-in. by 0.005-in. slit is cut parallel to the cylinder axis by the Elox (electrical discharge) process.

[16] J. M. Hendrie, J. Chem. Phys. **22**, 1503 (1954). See Ref. 1 HI, Sec. 21.

[17] A useful reference on high-temperature pyrometry is *Temperature-Measurement and Control*, edited by F. G. Brickwedde (Reinhold Publishing Company, New York, 1962). See Sec. IX in Part I.

The H beam passes through an adjustable collimating slit S and enters the electron gun, where it is bombarded by ≈ 13 V electrons perpendicular to the beam. The gun is a simple diode. It is mounted inside an electromagnet run at 575 G. This field collimates the electron beam and also provides β quenching. With its separate electromagnet, the gun is isolated from the Helmholtz coil which provides the magnetic field for the crossing-point experiment. This has the advantage of making the metastable beam production independent of the coil field setting during the crossing-point measurement.

The α beam from the gun passes through the flopper F. This is a solenoid covered with several layers of Netic and Co-Netic magnetic shielding. The shielding reduces stray fields to <1 G over a 1 cm axial length. A small solenoid current reduces this field to a small negative value with respect to the axial field of the Helmholtz coil. In the flopper, the α's undergo nonadiabatic transitions (Majorana flop),[18] and $\frac{1}{3}$ of them are converted to the state β_B.

Next, the beam travels down the axis of the Helmholtz coil. The coil provides the crossing-point field, *parallel* to the beam trajectory. This geometry avoids beam quenching by motional electric fields. The electrostatic shield E is a cylinder whose interior is polished and gold-plated to reduce quenching by stray fields. Collimating caps C_1 and C_2 define a beam size of 6.8 mm diam in the quenching region Q. Here, at the center of the coil, we apply a well-localized electrostatic quenching field perpendicular to the beam. This field is appreciable only over dimensions ~ 1 cm. P is a nuclear magnetic resonance (nmr) probe which is inserted into the experimental volume Q to measure the magnetic field.

After leaving the coil, the beam strikes the detector.[19] This is an untreated nickel surface which accepts all atoms passing through caps C_1 and C_2. A fraction of the $2S$ atoms in the beam ejects electrons.[20] An iron cylinder around the detector collects the electrons, and also shields the detector from the Helmholtz coil field. The electron current is amplified by an electrometer tube and monitored by a galvanometer.

The total $2S$ beam is measured by the galvanometer deflection resulting when a large quenching field ≈ 80 V/cm is applied to the beam at Q. This field quenches all $2S$ atoms. Such a galvanometer deflection is called the "beam flop." The total galvanometer signal contains small contributions from metastable H_2 and[21] from Lyman-α radiation produced in the electron gun. Neither gives a beam flop. A small beam flop comes from Lyman-α radiation produced at Q. This reduces the observed $2S$ quenching, and is spurious in terms of

TABLE I. Typical operating conditions.

Source chamber pressure	3×10^{-5} mm
Detector chamber pressure	8×10^{-7} mm
Oven temperature	3000°K
Oven pressure	1 mm
% dissociation	96%
Bombardment current	1000 μA
Bombardment current density	0.2 A/cm^2
Excitation voltage	12.8 V
Electrometer grid resistor	5×10^{11} Ω
Circuit time constant	5.2 sec
Detector sensitivity	1.06×10^{-16} A per mm galvanometer deflection
Observed $2S$ detector current	2.5×10^{-13} A
Observed noise (beam on)	1.2×10^{-16} A
Estimated *total* $2S$ yield[a]	2.4×10^{7}/sec

[a] Assumed detector efficiency is 6.5%. See W. L. Lichten and S. Schultz, Ref. 23.

counting $2S$ atoms. However, as shown by Lamb,[22] this effect does not enter when we measure *fractional* quenching (i.e., beam flop divided by total beam).

With the known $2S$ excitation cross section,[23] and reasonable values for various parameters,[24] the estimated $2S$ yield is within a factor of two of the observed signal. Beam shot noise and detector thermal noise entirely account for the observed beam noise. Typical operating conditions are listed in Table I.

B. Details of Helmholtz Coil Magnetic Field

A Helmholtz coil provides a longitudinal field for the crossing-point experiment. This choice of geometry avoids beam quenching by motional electric fields, and reduces the Stark shift due to these fields to a negligible value. The coil is enclosed in a vacuum-tight, water-cooled copper container filled with He to promote cooling. Coil power is supplied by a current-regulated supply with a stability of 5 ppm. The coil gives 1.66 G/mA at center.

During the experiment, the coil field is measured with the nmr probe P. This probe is approximately the same size as the region Q where most ($\approx 95\%$) of the quenching takes place. The nmr sample is a solution of water and $FeCl_3$. At a concentration of 2×10^{18} Fe^{3+} per cm^3, paramagnetic corrections are negligible.[25] Corrections due to bulk diamagnetism are <1 ppm.[26] To detect the proton nmr, field modulation is provided by applying a small 60 cps signal to the reference circuit in the coil power supply. Near the crossing-point field (605 G), the nmr center can be located and measured to better than 10 ppm.

[18] See discussion in N. F. Ramsey, *Molecular Beams* (Clarendon Press, Oxford, England, 1956), 1st ed., Chap. V.

[19] We note that only about 0.05% of the metastable beam is lost by natural decay over the 40-cm beam pathlength.

[20] This method of detection is described in HI, Ref. 1, Sec. 11. A later reference is H. D. Hagstrum, J. Appl. Phys. **31**, 897 (1960).

[21] W. L. Lichten, Phys. Rev. **120**, 848 (1960).

[22] See HIII, Ref. 1, Sec. 67.

[23] W. L. Lichten and S. Schultz, Phys. Rev. **116**, 1132 (1959). See also R. F. Stebbings, W. L. Fite, D. G. Hummer, and R. T. Brackmann, Phys. Rev. **119**, 1939 (1960).

[24] These are detailed in HI, Ref. 1, Sec. 12.

[25] We calculate the correction due to bulk paramagnetism to be <0.1 ppm. See W. C. Dickinson, Phys. Rev. **81**, 717 (1951).

[26] For a concise discussion of such corrections, see E. R. Andrew, *Nuclear Magnetic Resonance* (Cambridge, University Press, New York, 1958), 1st ed., Chap. 4.
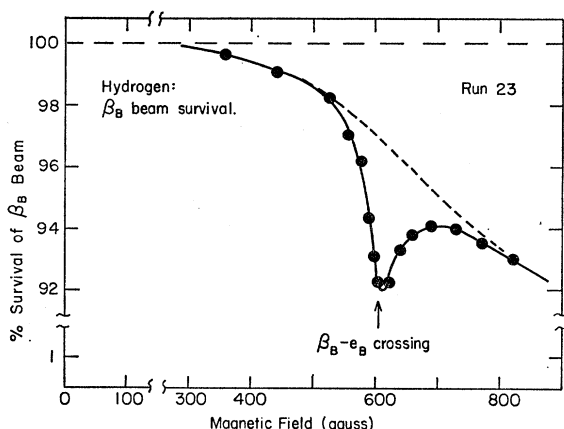
FIG. 5. Survival of a β_B beam as a function of magnetic field. The "beam notch" at the β_B-e_B crossing is caused by Stark quenching from stray fields and motional fields. The dashed line is an estimate of the motional field quenching.

Before and after the final runs, the coil field homogeneity was checked by a field plot using a small nmr probe. With proper shimming,[27] the field shows a slight droop at coil center, amounting to 60 ppm peak to peak (field second derivative >0 at coil center). No significant field gradients are present (first derivative <10 ppm/cm). Transverse homogeneity is 30 ppm over the beam cross section. During the final runs, the field homogeneity was checked by measuring the nmr linewidth. This remained constant at 35 mG. It compares with a calculated value of 19 mG.[28] The broadening is mainly due to the field variation over the experimental volume Q, and confirms the measured field characteristic.

C. Details of Quenching Field

The electrostatic quenching field is provided by electrodes located along a line through the coil center and perpendicular to the coil axis, spaced 5 mm on either side of that axis. The electrodes are polished and gold-plated to reduce stray fields. The quenching field is turned on by applying a dc voltage between the electrodes. One electrode is positive and the other negative with respect to electrical ground. The dimension over which this field is appreciable defines the quenching region Q.

It is important to design Q to be the same "size" as the homogeneous magnetic field region which is sampled by the nmr probe P. Otherwise, appreciable quenching takes place outside P, where the magnetic field is not measured and where it decreases rapidly. As we show in Appendix II, this leads to a line shift and line asymmetry. To avoid this, with our coil, we must localize Q to dimensions on the order of 1 cm.

Field characteristics of the electrodes were measured in an electrolytic tank. The fractional line center shift

[27] M. W. Garrett, J. Appl. Phys. **22**, 1091 (1951).
[28] This is calculated from the relaxation time determined by the Fe^{3+} concentration. See E. R. Andrew, Ref. 26, Chap. V.

(upward) for a particular quenching field is[29]

$$A = (144/125) \int_{-\infty}^{+\infty} E^2 \xi^4 d\xi \Big/ \int_{-\infty}^{+\infty} E^2 d\xi. \quad (1)$$

Here ξ is the distance along the coil axis normalized to the coil mean radius, with $\xi=0$ at coil center, and E is the quenching field along the coil axis. Measurement of E as a function of ξ gives A by numerical integration.

The electrodes are a pair of bars, each 9 mm high and 2 mm wide, mounted in front of a grounded disk 10 mm in diameter. Mounted 10 mm apart, these give an electric field which falls off at large ξ as ξ^{-4}. Less than 5% beam quenching occurs outside a region Q of size ~ 1 cm. This corresponds to $A \lesssim 26$ ppm. Over the beam cross section, the field is perpendicular to the coil axis, and constant to about 20%. The field at center is about 0.4 V/cm/volt of applied potential difference.

In summary, we have described an apparatus for producing and detecting a beam of metastable $2S$ hydrogen atoms. The *single* hfs component $\beta_B(m_I = -\frac{1}{2})$ of the state $\beta(m_J = -\frac{1}{2})$ can be produced. This state can be brought to the β_B-e_B crossing point by a magnetic field *parallel* to the beam trajectory. An experimental volume is provided where the β_B atoms can be quenched under controlled conditions by a well-localized electrostatic field. The quenching occurs in a region where the magnetic field is uniform and accurately measured.

III. PROCEDURE AND RESULTS

In this section, we discuss the measurements we have made. At the beginning of a run, the beam is stabilized in two ways. First, the oven is set to a temperature on the plateau of the dissociation curve. Second, the beam is bombarded at the voltage corresponding to the maximum of the excitation function. The beam stabilizes after a 1 h warmup period.

A. Beam Survival

Our first concern is whether a beam of β's can survive passage through the crossing-point magnetic field. A fraction of the beam is unavoidably lost by motional field quenching of off-axis beam atoms moving through transverse components of the coil field. This is reduced by defining a beam diameter small compared to the coil radius. Further beam loss occurs by quenching due to stray fields (from contact potentials, etc.) along the beam path. This is reduced by providing a gold-plated beam environment.

Figure 5 shows the survival of a β_B beam as a function of magnetic field. We estimate that about half of the 8% "beam notch" at the β_B-e_B crossing is caused by motional field quenching (dashed line). The remaining

[29] See Appendix II. We note that A is the largest experimental correction to the line center.

beam loss is due to stray fields.[30] The beam notch varies slightly from run to run, but not during a run. If the beam notch were included in a quenching line shape, it would asymmetrize the line. However, as we show in Appendix II, this asymmetry is removed by working with *fractional* quenching.

B. Beam Quenching

Our goal is to measure the β_B-e_B crossing-point magnetic field H_{CB} by finding the center of the β_B-e_B quenching resonance. The resonance line shape (Fig. 3) is observed by measuring fractional β_B quenching as a function of magnetic field. Fractional quenching is the β_B beam flop, caused by applying a small fixed voltage $V = V_W$ to the quenching electrodes, divided by the total β_B beam. Choice of a "working quench voltage" V_W determines the quenching maximum at H_{CB}. The total β_B beam is measured at each field by observing the beam flop caused by a voltage large enough to quench all β_B atoms. Thus we must study beam quenching before making any line shape or line center measurements.

We study beam quenching by measuring beam flop as a function of quenching voltage V at fixed magnetic field H. Let B be the galvanometer signal arising from the β_B beam arriving at the detector.[31] Beam flop as a function of V and H is

$$\Delta B(V,H) = B(0,H) - B(V,H). \qquad (2)$$

A measurement of ΔB versus V^2 produces a curve as in Fig. 6. From the Bethe-Lamb theory of the lifetime of the $2S$ state in external fields,[32] we can show (see Appendix II)

$$\Delta B(V,H) = B_T(H)\{1 - \exp[-V^2 f(H)]\}. \qquad (3)$$

$B_T(H)$ is the total β_B beam at field H. $f(H)$ has a Lorentzian resonance at $H = H_{CB}$, which makes ΔB resonant at the crossing point. But here, with H held constant, $f(H)$ is merely a constant characteristic of the quenching geometry. A theoretic fit of ΔB versus V^2 gives this constant, and allows a determination of the average quenching field E per unit V. In this way, from the beam quenching itself: $E/V \approx 0.4(\text{V/cm})/\text{V}$.

At low V, ΔB shows the expected linear dependence on V^2. Stray fields, on the order of 0.1 V/cm (from contact-like potential differences on the quenching
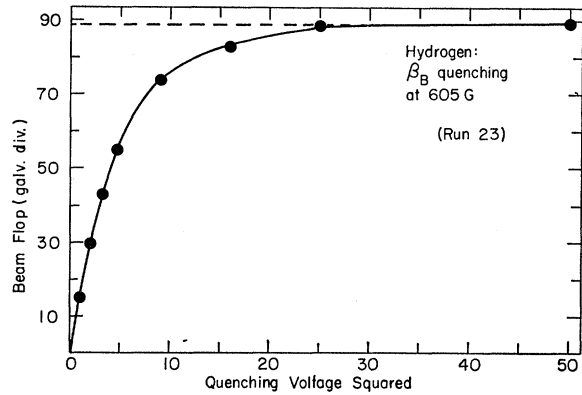

FIG. 6. Quenching of the metastable state β_B as a function of the voltage applied to the quenching electrodes. The electric field is about 0.4 V/cm/V of applied potential. Extrapolation of the beam flop "plateau" to zero volts (dashed line) gives the total β_B beam.

electrodes),[33] are detectable here by reversing the quenching voltage polarity. At high V, the β_B-e_B quenching saturates, and ΔB approaches a "plateau." The plateau slopes gradually upward, owing to a small contribution from α-f quenching.[34] Extrapolating the plateau to $V = 0$ (dashed line in Fig. 6) gives the total β_B beam $B_T(H)$.

The total beam, α's and β_B's, is measured by taking a plateau at large quenching fields, $V \sim 200$ V. We find the β_B fraction is 0.33 ± 0.02. This agrees with the simple expectation that in the flopper the α's are equally distributed among the three $F = 1$ zero-field states. We test the beam emerging from the electron gun for the unwanted β_A component as follows. The flopper is withdrawn from the beam path and the coil field is set to the β_A-e_A crossing point, $H = H_{CA} \approx 542$ G. Here β_A's are detected most easily. ΔB versus V^2 is measured for low V. The small beam flop observed can be fully accounted for by α-f quenching. This experiment determines an upper limit on the number of β_A's present. In this way, the α beam is found to contain a β_A fraction $< 5 \times 10^{-5}$. With negligible β_A regeneration in the flopper,[35] we estimate that the regenerated β_B component contains < 2 parts in 10^4 of β_A contamination. This contributes a negligible shift to the β_B quenching peak.

C. Line Shape

From $\Delta B(V,H_{CB})$ versus V^2, we choose a working quench voltage $V_W \approx 1.5$ V which gives a maximum

---

[30] From the notch, we estimate stray fields are < 0.2 V/cm. However, if we claim that no stray fields are present, then less than 5% of the β_B's are "unaccountably" lost upon passage through the crossing-point field. This can be used to establish a new upper limit for the $2P_{1/2}$ parity impurity in the $2S_{1/2}$ state. If the $2S$ state is: $\phi_S' = \phi_S + \mu\phi_P$, where ϕ_S and ϕ_P are pure S- and P-wave functions, then by this experiment $|\mu|^2 < 2 \times 10^{-8}$, at zero magnetic field. This is to be compared with $|\mu|^2 < 7 \times 10^{-7}$, obtained by W. L. Fite, R. T. Brackmann, D. G. Hummer, and R. F. Stebbings, Phys. Rev. 116, 363 (1959).

[31] At the quenching voltages used, the α component of the beam contributes an almost negligible beam flop. We neglect the α beam here, and correct for it later (in Appendix II).

[32] See Ref. 14.

[33] This was noted also in HIV, Ref. 1, Sec. 73.

[34] Electric field E perpendicular to magnetic field H induces α-f as well as β-e transitions. The α-f quenching is very small however, because of the large α-f separation (about 2200 Mc/sec near H_{CB}). α-e and β-f quenching, caused by E parallel to H, are negligible for our electrode geometry. α-f quenching corrections are made in Appendix II.

[35] At $H = 0$, $\beta_A(m_I = +\frac{1}{2})$ is separated from $\beta_B(m_I = -\frac{1}{2})$ by 177 Mc/sec. In our flopper, the Majorana transitions have a calculated half-width of about 1 Mc/sec. From this, we estimate the ratio of β_A to β_B regeneration to be less than 10^{-5}.

TABLE II. Line-shape data.

Run	F_M	Half-width (G)		Width at working points (G)	% quench at working points		Slope at working points (kc/%)	
		Exp.	Theoret.		Exp.	Theoret.	Exp.	Theoret.
15a	0.47	65.4	63.4	33.3	37.4	37.0	4.92	4.34
15b	0.47	65.4	63.4	66.5	23.0	22.6	6.66	6.00
16	0.47	68.1	63.4	43.2	33.3	33.6	5.13	4.60
17	0.415	65.2	62.0	43.2	28.7	28.2	5.31	5.07

fractional β_B quenching ≈ 0.40-0.50. The β_B-e_B quenching line shape is taken at constant V_W by measuring fractional quenching

$$F(V_W,H) = \Delta B(V_W,H)/B_T(H), \qquad (4)$$

versus H. ΔB is the average galvanometer deflection for two "quench on" $(V=V_W)$ and one "quench off" $(V=0)$ readings, taken at 20-sec intervals. B_T is obtained from a β_B plateau established at each field measurement point. We get the plateau by measuring ΔB at voltages V_P, $\sqrt{2}V_P$, and $2V_P$, with V_P chosen to lie just above the "knee" of the quench plateau.[36] To get a line shape, the quenching is measured at the maximum, $F_M = F(V_W, H_{CB})$, and then at symmetric points above and below H_{CB}.[37] The magnetic field is measured by proton nmr after each fractional quenching determination.

Such a line shape is shown in Fig. 3. To good approximation, the line shape is

$$F(r) = 1 - \exp[\ln(1-F_M)/1+\kappa_0{}^2(1-r)^2] \qquad (5)$$

as we show in Appendices I and II. Here, $r = H_0/H_{CB}$, H_0 the coil central field. $\kappa_0 = 4\pi\tau_P S_B \approx 22$, where $\tau_P = 1.6 \times 10^{-9}$ sec is the e_B lifetime and $S_B = 1117$ Mc/sec is the β_B-e_B separation at zero field. F_M is the observed quenching maximum, determined by choice of working quench voltage V_W.[38] Neglected here are several corrections which make F asymmetric about $r=1$. These are discussed in Appendix II. They are important only for corrections ~ 1 part in 10^4 to precision measurement of the line center.

The experimental points in Fig. 3 are compared with $F(r)$ for an observed $F_M = 0.415$. The measured half-width is 65 G, as compared with the value 62 G calculated from the theoretical line shape. Line centers, taken as midpoints between symmetric pairs of experimental points, increase by less than $+4$ parts in 10^4 from top to bottom of the line. This agrees in sign and magnitude with the expected total line asymmetry.

Two other detailed line shapes exhibit the same features.

A simplified version of the Bethe-Lamb theory is used to describe the line shape and to check for line asymmetry. Such line-broadening effects as nonuniform quenching over the beam cross section (Sec. IIC), and an average over the beam velocity distribution, are not taken into account.[39] The over-all line shape agreement is considered reasonable confirmation of the Bethe-Lamb theory.

Table II compares three experimental line shapes with the simple theory. F_M is the observed maximum quenching. The half-width is calculated from $F(r)$ (see Fig. 8, Appendix I). The "working points" are symmetrical points on the line shape between which line centers are measured. For these points, percentage quenching and slope are calculated from $F(r)$. The slope is $(dF/dr)^{-1}$, given in units of proton nmr frequency per percent quenching of the β_B beam.

D. Line Centers

Measurements

For line-center measurements, we choose working points at $H_\pm = H_{CB} \pm \Delta H$, near the inflection points of the nearly Lorentzian line shape. Typically, the working points are at 30% quenching ($\frac{3}{4}$ of maximum quenching), with linewidth $2\Delta H \approx 40$ G. At the beginning of each run, the line shape is measured near $H_\pm$ to establish line slopes at the working points. Line slopes at $H_\pm$ are the same to within 2% measuring error, again indicating no apparent line asymmetry.

Alternating between $H_\pm$, we measure fractional quenching $F_\pm$. At each working point, the measurement

---

[36] As we depart from H_{CB}, the β_B's become progressively harder to quench, and V_P must be chosen larger so as to lie at the same relative position on the plateau. Over $H_{CB} \pm 20$ G, $V_P = 6$ V, while at $H_{CB} \pm 75$ G, $V_P = 12$ V.

[37] This avoids line-shape distortion from field drift due to coil thermal expansion. This drift is <20 ppm during the time of the F measurement.

[38] Relating F_M to V_W (see Appendix II), we confirm the quenching constant: $E/V \approx 0.4$ (V/cm)/V, as found in Sec. IIIB.

[39] Since the observed total line asymmetry agrees with that expected from the simple line-shape theory (Appendices I and II), we are convinced that all important asymmetry effects tending to shift the observed line center have been accounted for. Effects which broaden the line without asymmetrizing it can then be ignored. Their inclusion in the line-shape theory would only complicate the analysis, without significantly affecting the calculated shift correction (Sec. IIID). This is the case with the effects mentioned above. Nonuniform quenching gives no line asymmetry. Although the velocity distribution depends upon magnetic field whenever motional Stark quenching is important (see HV, Ref. 1, Appendix VII), this effect is very small in our experiment, and the velocity averaging leads to negligible asymmetry. Neither effect shifts the line center. On the other hand, both effects tend to broaden the line. A rough calculation shows that they can increase the linewidth by several percent. We are reasonably certain that they account for the discrepancy between the observed linewidths and those calculated from the simple theory (Table II).

sequence is: Proton nmr measurement of field, beam flop ΔB at the working voltage V_W (average of three quench-on and two quench-off readings), quench plateau to determine the total β_B beam B_T for normalization purposes, ΔB again, nmr again. Total measurement time is about 10 min. Field drift during the ΔB measurement is less than 10 ppm. From this set of measurements, we get two determinations of fractional quenching at a measured field. The sequence is repeated at the other working point. Pairing the $\Delta B/B_T$ values, we get two sets (F_+, F_-), with corresponding nmr frequencies (ω_+, ω_-). Assuming a symmetric line, we take the line center

$$\omega_{CB}' = \tfrac{1}{2}(\omega_+ + \omega_-) + \tfrac{1}{2}(F_+ - F_-)(dF/d\omega)_{av}^{-1}. \quad (6)$$

Here $(dF/d\omega)_{av}$ is the average of the experimentally measured slopes at $H_\pm$. With a steady beam, and careful pre-setting of H_{CB}, the "noise" term is normally $<4 \times 10^{-4}\omega_{CB}'$.

A run consists of 16 to 20 measurements of the line center ω_{CB}'. In seven runs, we have 124 measurements. Figure 7 is a histogram of these. The centers here are corrected by ~ 1 part in 10^4, as explained in the following section.

Corrections Used

As we show in Appendix II, the real line shape is

$$F'(r) = \lambda(r)\left\{1 - \exp\left[\frac{\ln(1 - F_M')}{1 + \kappa_0^2(1 - r)^2}K(r)\right]\right\}, \quad (7)$$

which is to be compared with Eq. (5). λ and K are factors which account for line asymmetries. They shift the observed line center from the true center at $r = 1$. λ accounts for errors in B_T from the plateau extrapolation, and also for contributions from α-f quenching. At the working points, λ alone gives a shift of -10 ppm.[40] K includes the "natural" corrections due to Stark matrix element variation and Zeeman curvature of the $2P$ level e_B, as well as a correction due to the finite size of the quenching region (Sec. IIC). At the working points, K alone gives a line center shift of $+100$ ppm. Numerical values for λ and K are given in Appendix II, Fig. 9.

We correct the observed line center ω_{CB}' by subtracting

$$\Delta\omega = \tfrac{1}{2}(F_+' - F_-')(dF/d\omega)_{av}^{-1}. \quad (8)$$

Here, F' is calculated at the working points from Eq. (7). For example, in run 23a (Table III), $F_M' = 0.42$ and the working points are at $\Delta H = 20$ G. We calculate $(F_+' - F_-')/2 = 5.3 \times 10^{-2}\%$. With the measured working point slope $(dF/d\omega)_{av}^{-1} = 5$ kc/%, we get $\Delta\omega = 265$ cps. The net correction is $1.02 \times 10^{-4}\omega_{CB}'$. In calculating the Lamb shift S from the corrected line center ω_{CB}

---

[40] As we show in Sec. IV the line center is (very nearly) linearly related to the Lamb shift S. Thus, a 10 ppm correction to the observed line center gives the same relative correction in S.
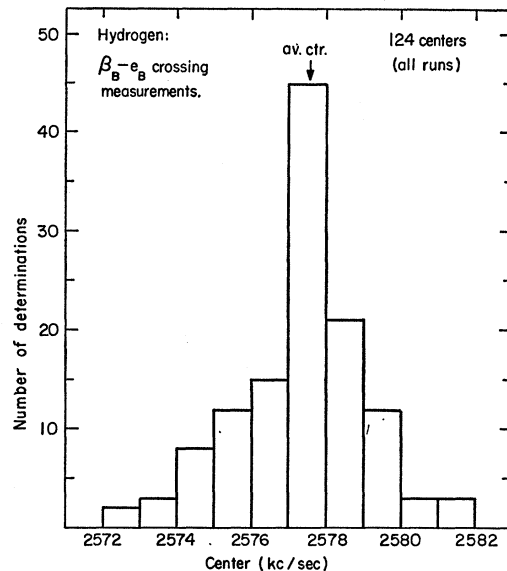

FIG. 7. Histogram of measurements of the center of the β_B-e_B quenching line shape. The magnetic field at center is measured by proton nmr frequency in water. All centers here have been corrected by about -1 part in 10^4.

$= \omega_{CB}' - \Delta\omega$, we thereby correct S by about 1 part in 10^4. This is to be compared with the Lamb experiments, where S (in hydrogen) was corrected by more than 1 part in 10^3.[41]

Other Corrections

In addition to the corrections used above, a number of other factors may asymmetrize the line and shift the observed line center ω_{CB}'. They are: coil field inhomogeneity, β_A impurity in the β_B beam, magnetic field dependence of the beam velocity distribution, Stark shifts (due to the motional field and to the applied quenching field), forbidden transitions (with $\Delta m_I \neq 0$),[42] β-f and α-e quenching contributions. We estimate the net correction from these effects to be <10 ppm.

Results

Table III gives the results of line center measurements for seven independent runs. ω_{CB}' is the observed average proton nmr frequency (in water) at the center

---

[41] See HV, Ref. 1, Tables XX and XXI.

[42] See HIV, Ref. 1, Sec. 74. No direct $\Delta m_I \neq 0$ transitions occur in our experiment, since we work with the "pure" hfs state $\beta_B(m_F = -1)$. However, $e_B(m_F = 0)$ is coupled to $\beta_A(m_F = 0)$ via the hfs interaction [e_B to $f(m_F = 0)$, β_A to $\alpha(m_F = 0)$] followed by Stark coupling due to that component of the electric field *parallel* to the magnetic field [$(f(m_F = 0)$ to β_A, $\alpha(m_F = 0)$ to e_B]. This perturbs the e_B energy level and shifts the apparent β_B-e_B crossing point. An estimate based upon Eq. (215) of HIII, Ref. 1, shows that crossing point B is shifted downward by a fractional amount $\sim 10^{-7}F^2$, where F is the parallel electric field in V/cm. We estimate that, at most, F could be a few tenths of a V/cm, either from stray fields (Sec. IIIA), or from a σ component of our predominantly π quenching geometry (Sec. IIC). Consequently, the shift due to F is negligible. We are indebted to Professor R. Novick for pointing out this effect.

TABLE III. Line-center data.

Run	Number of centers	Average center ω_{CB}', kc/sec	Correction $\Delta\omega$, ppm	rms error σ_r, kc/sec	Fractional weight, f_r
15	16	2577.323	121	0.414	0.032
16	20	2577.342	122	0.485	0.024
17	20	2577.507	115	0.384	0.038
20a	12	2578.285	91	0.788	0.009
20e	20	2577.127	91	0.479	0.024
23a	18	2578.042	102	0.117	0.411
23e	18	2577.765	102	0.110	0.462

of the β_B-e_B quenching peak. $\Delta\omega$ is the calculated correction of Eq. (8). σ_r is the rms error of the mean in run r. The fractional weight f_r is proportional to σ_r^{-2}.

The corrected center is $\omega_{CB}=\omega_{CB}'-\Delta\omega$. The weighted average corrected center for all runs is

$$\omega_{CB}=2577.57\pm0.25 \text{ kc/sec}, \qquad (9)$$

which corresponds to a crossing point field $H_{CB}=605.38$ ±0.06 G. Internal precision of the data is $\sigma_I=29$ ppm, which is consistent with the external precision $\sigma_E=37$ ppm.[43] The quoted error is about three times the rms precision of the weighted mean of the means.

In this section, we studied accidental beam quenching by both stray and motional electric fields, as well as by the controlled quenching field in the experimental volume Q. The beam was analyzed for various metastable components. We described the measurement of the β_B-e_B quenching line shape and compared it with a simple version of the Bethe-Lamb theory. Measurements of the line center were described and various line-asymmetry corrections, amounting to about -1 part in 10^4 of the observed line center, were discussed. We presented the results of 124 measurements of the line center, and arrived at a weighted average corrected center for the β_B-e_B crossing point field.

IV. CALCULATION OF THE LAMB SHIFT

In this section, we calculate the Lamb shift S from the β_B-e_B crossing-point field as measured by the proton nmr frequency ω_{CB}. To do this, we use the nonrelativistic Breit-Rabi formula[44] for the β-e frequency separation. Treating hfs as a perturbation, we obtain the β_B-e_B separation as a function of magnetic field. Setting this equal to zero at the crossing point, we relate ω_{CB} to S. Using a diamagnetic correction for protons in water, and the accurately known $2S$ hfs interval, we calculate S from ω_{CB}.

In the calculation, we include the anomalous part of the electron spin g-value g_S. The orbital g value is

corrected to: $g_L=1-(m/M)$, where m/M is the electron-proton mass ratio.[45] We use Lamb's hfs corrections, after we have corrected an error.[46] For numerical calculations, we use the 1955 Atomic Constants,[47] and the experimental values of the $2P_{3/2}$-$2P_{1/2}$ fs interval ΔE,[48] and $2S_{1/2}$ hfs interval Δw.[49]

With $\mu_0=e/4\pi mc$, and the dimensionless magnetic field variable

$$x=(g_S-g_L)\mu_0 H/\Delta E, \qquad (10)$$

the β-e frequency separation is

$$\nu=S-\tfrac{1}{2}(g_S+g_L)\mu_0 H+\tfrac{1}{2}\Delta E[(1+\tfrac{2}{3}x+x^2)^{1/2}-1]. \quad (11)$$

Here, $g_S=2(1+a)$, where a is the anomalous part of the electron moment,[50] and $g_L=1-(m/M)$.

To get the β_B-e_B separation, we add the correction

$$\delta\nu_B=\tfrac{1}{3}\Delta w-(1/36)(\Delta w)^2/g_J\mu_0 H+(1/72)$$
$$\times(g_S-g_L)(\Delta w/\Delta E)\mu_0 H, \quad (12)$$

to ν of Eq. (11). The first term is the hfs contribution for complete I-J decoupling. We have assumed here that the $2P_{1/2}$ hfs interval is exactly $\Delta w/3$. The second term corrects for hfs curvature (incomplete I-J decoupling) near the β_B-e_B crossing point. It is the leading term in a high-field Breit-Rabi expansion of the hfs energy.[51] The next term in this expansion is of relative order 3×10^{-3} near the crossing point, which decreases the calculated S by about 4 ppm. g_J is the Lande g value for $2P_{1/2}$; $g_J=\tfrac{2}{3}$ to requisite accuracy. The last term in Eq. (12) is a correction for L-S decoupling.[52]

The β_B-e_B separation is $\nu+\delta\nu_B$, which is

$$\nu_B=S_B-\tfrac{1}{2}\Delta E\{T_Bx-[(1+\tfrac{2}{3}x+x^2)^{1/2}-1]\}$$
$$-(1/24)(\Delta w)^2/\mu_0 H, \quad (13)$$

where $S_B=S+\Delta w/3$, and

$$T_B=(g_S+g_L)(g_S-g_L)^{-1}-(1/36)(\Delta w/\Delta E). \quad (14)$$

At the β_B-e_B crossing point, we set $\nu_B=0$.[53] This relates our measured line center ω_{CB} to the Lamb shift S. If we use Eq. (13) directly, the conversion equation intro-

---

[43] We define $\sigma_I=[\Sigma_r(f_r\sigma_r)^2]^{1/2}$, and $\sigma_E=[\Sigma_r f_r\delta_r^2/(R-1)]^{1/2}$. Here, $\delta_r=\omega_{CB}(r)-\omega_{CB}$, and $R=7$ is the number of runs.

[44] For a discussion of relativistic corrections, see HIII, Ref. 1, Sec. 54a, and Sec. 47 in BS(57), Ref. 3. The relativistic Breit-Rabi formula is given in M. E. Rose, *Relativistic Electron Theory* (John Wiley & Sons, Inc., New York, 1961), 1st ed., p. 185. For the present problem, we estimate that for given ω_{CB}, relativistic corrections lower our calculated S by about 7 ppm.

[45] M. Phillips, Phys. Rev. 76, 1803 (1949). Also see HIII, Ref. 1, Sec. 54d.

[46] The hfs corrections are given in HIII, Ref. 1, Sec. 56. Equation (184) should have a coefficient 1/32 rather than 1/64. As discussed in Sec. V, this error may change Lamb's value for S by a significant amount.

[47] E. R. Cohen, J. W. M. Dumond, T. W. Layton, and J. S. Rollett, Rev. Mod. Phys. 27, 363 (1955). A later reference is J. W. M. DuMond, Ann. Phys. 7, 365 (1959).

[48] See HVI, Ref. 1, Sec. 109. Convert ^{2}H to ^{1}H value by: $\Delta E(1)=(R_1/R_2)\Delta E(2)$, $R=$Rydberg. R_1/R_2 uncertainty is <0.2 ppm (see Ref. 47). The result is: $\Delta E=10968.61\pm0.2$ Mc/sec

[49] J. Heberle, H. Reich, and P. Kusch, Phys. Rev. 101, 612. (1956). The result is $\Delta w=177.55686$ (±0.3 ppm) Mc/sec.

[50] As measured, $a=(1.159622\pm23$ ppm$)\times10^{-3}$. See D. T. Wilkinson and S. R. Crane, Ref. 6.

[51] By Eq. (184) in HIII, Ref. 1, this term has a numerical coefficient 1/72, which is too small by a factor of 2.

[52] See HIII, Ref. 1, Sec. 56b. We note that Eq. (182) is also too small by a factor of 2. However, we agree with Lamb's g_I correction.

[53] For Lamb's value of S (Ref. 12), we calculate the crossing-point field $H_{CB}=605.21\pm0.06$ G. The uncertainty is mainly from S.

duces an 18 ppm intrinsic uncertainty in S_B, due to uncertainty in ΔE. To reduce this, define

$$L(x) = \tfrac{1}{2}\left[(1+\tfrac{2}{3}x+x^2)^{1/2} - (1+\tfrac{1}{3}x)\right] \xrightarrow[x \ll 1]{} \tfrac{2}{9}x^2. \quad (15)$$

Using $L(x)$ in the $\nu_B = 0$ equation, we thereby reduce the intrinsic uncertainty from ΔE to less than 0.2 ppm.

With ω_{CB} the measured line center nmr frequency, the β_B-e_B crossing-point field is $H_{CB} = \omega_{CB}/2\mu_P'$. μ_P' is the proton magnetic moment (in frequency units) in water. Convert μ_P' to μ_P for a free proton by: $\mu_P' = (1-\sigma)\mu_P$, where $\sigma = 27.8 \times 10^{-6}$ is the diamagnetic shielding correction in water.[54] Then at the crossing point

$$x_{CB} = (k/\Delta E)\omega_{CB}, \quad k = \tfrac{1}{2}(g_S - g_L)(1-\sigma)^{-1}(\mu_0/\mu_P). \quad (16)$$

Write $\mu_0/\mu_P = (1+a)^{-1}(g_S/g_P)$, where a is the anomalous part of the electron moment.[50] g_S/g_P is the free electron-free proton g-value ratio.[55] From this, with ω_{CB} in Mc/sec, we calculate the numerical values

$$x_{CB} = (3.00570 \pm 18 \text{ ppm}) \times 10^{-2}\omega_{CB},$$

$$b = \tfrac{1}{2}(T_B - \tfrac{1}{3})k = 438.3838(\pm < 2 \text{ ppm}). \quad (17)$$

Defining the numerical constant

$$\Omega = (1/24)(g_S - g_L)(\Delta w)^2/\Delta E = 0.120103 \text{ Mc/sec}, \quad (18)$$

we write the ω_{CB}-to-S conversion equation as

$$S + \Delta w/3 = b\omega_{CB} - L(x_{CB})\Delta E + \Omega x_{CB}^{-1}. \quad (19)$$

This allows a conversion with an estimated intrinsic accuracy of about 10 ppm.[56]

Table IV gives the calculated S for each of the seven runs in Table III. We calculate S from the corrected line center $\omega_{CB} = \omega_{CB}' - \Delta\omega$. The "correction" is the amount by which S is reduced from the value S' corresponding to ω_{CB}'. In each run, the uncertainty is the rms error of the mean.

Using the weighted average ω_{CB} of Eq. (9), we calculate

$$S = 1058.07 \pm 0.10 \text{ Mc/sec}. \quad (20)$$

This is the final result for the Lamb shift in this experiment. The uncertainty is approximately three times the rms precision.[57]

V. DISCUSSION

Table V compares our experiment with those of Dayhoff, Triebwasser, and Lamb.[58] In the present

TABLE IV. Calculated Lamb shifts.

Run	Fractional weight	Correction Mc/sec	Corrected Lamb shift S, Mc/sec
15	0.032	0.14	1057.85±0.17
16	0.024	0.14	1057.85±0.20
17	0.038	0.13	1057.93±0.16
20a	0.009	0.11	1058.27±0.32
20e	0.024	0.11	1057.80±0.20
23a	0.411	0.12	1058.16±0.05
23e	0.462	0.12	1058.05±0.05

experiment, the quenching line shape is relatively narrow. This is mainly due to the elimination of the hfs complication (Secs. IA and IB). Corrections due to Zeeman curvature and incomplete Back-Goudsmit effect are considerably reduced. As a consequence, the net correction to the observed S is relatively small.

Our result for S is 0.3 Mc/sec higher than the mean of Lamb's results. The reason for this discrepancy is not known. However, we have found an error in Lamb's hfs curvature corrections.[59] If this error carries through to the final corrections made on his observed S, it would change his quoted values for $S(\alpha e)$ and $S(\alpha f)$.[60] Correcting the error, we find new values for S (in hydrogen[61]) from the Lamb experiments

$$S'(\alpha e) = 1057.97 \pm 0.10 \text{ Mc/sec},$$

$$S'(\alpha f) = 1057.45 \pm 0.10 \text{ Mc/sec}. \quad (21)$$

The discrepancy here would suggest further systematic error. If so, $S'(\alpha e)$ would be more reliable than $S'(\alpha f)$, since its total correction is smaller. Within error limits, $S'(\alpha e)$ agrees with our result for S.

However, Lamb's values for $S(\alpha e)$ and $S(\alpha f)$ may be regarded as independent measurements of S, and since they show excellent internal agreement, it is possible that the erroneous hfs correction did not carry through to his final analysis. In this case, the 0.3 Mc/sec discrepancy between our result and Lamb's cannot be regarded as firmly established until the present value for S has been confirmed by an independent measurement. Our result, obtained from the isolation and measurement of crossing point B, should be checked by an independent measurement based upon the isolation and measurement of crossing point A (see Fig. 2).

---

[54] See Ref. 18, p. 165. Quoted accuracy in σ is 1.5%.

[55] $g_S/g_P = 658.2288$ (± 0.9 ppm). See S. Koenig, A. Prodell, and P. Kusch, Phys. Rev. 88, 191 (1952).

[56] Because we neglect relativistic and higher order hfs corrections, S calculated from Eq. (19) should be reduced by about 0.01 Mc/sec. This correction is made in Table IV.

[57] The precision indices are defined in Ref. 43. If, rather than weighting the data, we treated all data as equivalent, we would quote: $S = 1057.98 \pm 0.16$ Mc/sec, with consistencies $\sigma_I = \sigma_E = 60$ ppm. However, the weighting is preferred, in order to properly recognize the relatively high precision of runs 23a and 23e.

[58] See HV, Ref. 1, Tables XVII, and XXI.

[59] See Refs. 46 and 51. The error occurs in Lamb's analysis of the α-e and α-f hfs transition frequencies, $\nu_{\alpha e}(m_I)$ and $\nu_{\alpha f}(m_I)$. Correcting the error, we find $\nu_{\alpha e}(-\tfrac{1}{2})$ decreased by 0.40 Mc/sec, and $\nu_{\alpha f}(+\tfrac{1}{2})$ increased by 0.67 Mc/sec. This raises the center of the α-e quenching line shape by 0.22 G, and lowers the α-f center by 0.18 G.

[60] In HIV, Ref. 1, Table XIV, Lamb calculates the correction to $S(\alpha e)$. It is virtually impossible to tell if the incorrect hfs term is used. Furthermore, since the original calculations are no longer available, it is not possible to check if the error carried through to the final analysis. W. E. Lamb, Jr. (private communication).

[61] We note that the hfs error would not significantly change Lamb's results for S in D, $n = 2$, because the hfs there is much smaller. The correction would not be more than a small fraction of 0.1 Mc/sec.

TABLE V. Comparison of measured Lamb shifts in H, $n=2$.

Experiment	Levels mixed	Freq. Mc/sec	Center[a] H_c, G	Width[b] ΔH, G	Observed $\mathcal{S}$, Mc/sec	Correction Mc/sec	Quoted $\mathcal{S}$, Mc/sec
Lamb et al.	α-e	2195	1159.5	120	1059.03	-1.28	1057.75 ± 0.10
Lamb et al.	α-f	2395	703.7	104	1061.02	-3.22	1057.79 ± 0.10
Present exp.	β_B-e_B	0	605.4	40	1058.19	-0.12	1058.07 ± 0.10

[a] H_c is the magnetic field at the center of the quenching resonance.
[b] ΔH is the full linewidth at the line-center working points.

The most recent, published, theoretical value for $\mathcal{S}$ in H, $n=2$, is Layzer's calculation[62]

$$\mathcal{S}_{th}=1057.70\pm0.15 \text{ Mc/sec}, \qquad (22)$$

which takes into account terms of order $\alpha(Z\alpha)^6\ln^2(Z\alpha)$ and $\alpha(Z\alpha)^6\ln(Z\alpha)$. Layzer's values agree well with Lamb's results in both H and D. More recently, Erickson[63] has calculated an additional contribution of -0.13 Mc/sec from a term of order $\alpha(Z\alpha)^6$. Correction of some of the calculations prior to Layzer's give a value

$$\mathcal{S}_{th}'=1057.64\pm0.15 \text{ Mc/sec}. \qquad (23)$$

Calculations are still in progress. Terms of order $\alpha^2(Z\alpha)^4$ are being re-examined. Erickson informs us that the value in Eq. (23) will be changed by some fraction of a Mc/sec.[64]

Our value for $\mathcal{S}$, Eq. (20), is 0.43 Mc/sec higher than present theory, Eq. (23). Part of the difference may be due to uncalculated proton structure corrections, as mentioned by Salpeter.[65] If we use Fulton and Martin's result,[66] the theoretical Lamb shift difference between D and H is

$$\mathcal{S}(D)-\mathcal{S}(H)=(1.25-\epsilon_{st}'\pm0.035) \text{ Mc/sec}. \qquad (24)$$

ϵ_{st}' is a structure correction addition to $\mathcal{S}(H)$; it does not enter into the calculation of $\mathcal{S}(D)$. Using Lamb's value of $\mathcal{S}(D)$,[61,67] and our value of $\mathcal{S}(H)$, we get $\epsilon_{st}'=0.32\pm0.15$ Mc/sec. It would be surprising if the uncalculated proton structure corrections were this large. However, the large value of ϵ_{st}' calculated here may suggest that further proton structure effects are important. To check this, it is clear that the present technique should be used to remeasure $\mathcal{S}(D)$.

The present experiment indicates a new value for the Lamb shift in H, $n=2$, higher by about 0.3 Mc/sec than the result from the Lamb experiments. The importance of checking this discrepancy, in terms of a possible redetermination of the fine structure constant α, constitutes a basis for further experiments.

ACKNOWLEDGMENTS

APPENDIX I: THE QUENCHING RESONANCE

We apply the Bethe-Lamb theory[68] of the lifetime of the 2S state in external fields to the β_B-e_B quenching resonance. We show how a beam of β_B atoms is strongly quenched by small electrostatic fields near the β_B-e_B crossing point, at $H_{CB}\approx605$ G. We derive an approximate line shape formula, and calculate some relevant numbers.

We mix e_B with β_B by a "small" Stark matrix element V. With the natural decay rates $\gamma_S=8.226/\text{sec}$[69] for β_B and $\gamma_P=6.270\times10^8/\text{sec}$ for e_B, a time-dependent perturbation calculation gives the mixed β_B decay rate Γ_S. To second order in the perturbation parameter $q=2V/\hbar\gamma_P$

$$\Gamma_S=\gamma_S+\gamma_P|q|^2(1+\kappa^2)^{-1}, \qquad (A1)$$

for $2|q|\ll1$.[70] Here, $\kappa=2\delta E/\hbar\gamma_P$ is proportional to the unperturbed β_B-e_B energy difference $\delta E=E_S-E_P$.[71]

[62] See A. J. Layzer, Ref. 5. For calculations prior to this, see A. J. Petermann, Fortschr. Physik 6, 505 (1958).
[63] A preliminary summary of G. W. Erickson's results was presented at the Eastern Theoretical Physics Conference held at Chapel Hill, North Carolina, October 1963 (unpublished).
[64] G. W. Erickson (private communication).
[65] E. E. Salpeter, Phys. Rev. 89, 92 (1953). Such corrections (nucleon polarization terms and refinements in the finite-size corrections) are also mentioned by Greenberg and Foley (Ref. 4) as possible reasons for the hydrogen hfs discrepancy.
[66] T. Fulton and P. C. Martin, Phys. Rev. 95, 811 (1954). In Eq. (24), ϵ_{st}' is meant to be that part of Salpeter's ϵ_{st} beyond the contribution from the finite size of the proton, which was calculated to be $+0.12$ Mc/sec by W. Aron and A. J. Zuchelli, Phys. Rev. 105, 1681 (1957).
[67] See HV, Ref. 1, Sec. 94. Result is $\mathcal{S}(D)=1059.00\pm0.10$ Mc/sec.

[68] See Ref. 14. Also HIII, Ref. 1, Sec. 71.
[69] J. Shapiro and G. Breit, Phys. Rev. 113, 179 (1959).
[70] Under this condition the Wigner-von Neumann no-crossing theorem does not apply.
[71] It is worth noting here that the perturbed energy separation is $\delta E'=[1+2|q|^2(1+\kappa^2)^{-1}]\delta E$. Inclusion of $\delta E'$ rather than δE in the Γ_S denominator would not shift the resonance line center. It would be equivalent to a calculation to fourth order in q. This is not necessary for the low quenching fields used in this experiment.

For electric field parallel to the quantization axis (magnetic field direction), $V \equiv 0$. For a perpendicular field of size E

$$|q|^2 = C(E/E_0)^2,$$

$$E_0 = \hbar\gamma_P/2\sqrt{3}ea_0 = 22.5 \text{ V/cm}. \tag{A2}$$

E_0 is a scale field for β-e mixing which defines the relative size of the Stark perturbation. C is a correction to the matrix element, due to L-S decoupling by the magnetic field H. C increases slowly with H, from $C=1$ at $H=0$, to $C=C_B=1.05$ at $H=H_{CB}$. It is discussed in Appendix II.

The smallness condition on V is $E \ll 11.2$ V/cm. Take $E=1$ V/cm. At $H=0$, $\delta E/h = 1117$ Mc/sec and $\kappa = \kappa_L = 22.4$. The γ_P contribution to Γ_S is then about $315\gamma_S$, so that the P-decay mode predominates. To good approximation

$$\Gamma_S = C(E/E_0)^2(1+\kappa^2)^{-1}\gamma_P, \tag{A3}$$

over $0 \leqslant H \leqslant 2H_{CB}$, and for $0.1 \leqslant E \leqslant 11.2$ V/cm. Γ_S has a Lorentzian resonance at $\kappa=0$, and increases by a factor $1+\kappa_L^2 \approx 500$ from $H=0$ to $H=H_{CB}$. The resonance half-width is

$$\delta H_L = 2H_{CB}/\kappa_L = 54 \text{ G}. \tag{A4}$$

A beam B of β_B's decays as $dB/dt = -\Gamma_S B$. With ℓ the path length along the beam, $dt = d\ell/v$, where v is the average beam velocity. Let $\ell=0$ at coil center and define $\xi = \ell/R$ where $R=1.95''$ is the coil mean radius. The beam is

$$B = B_0 \exp\left[-(2R/v\tau_P)\int_0^\infty C(E/E_0)^2(1+\kappa^2)^{-1}d\xi\right], \tag{A5}$$

where $\tau_P = 1/\gamma_P$ is the e_B lifetime.[72] E is well localized at $\xi=0$ where C and κ vary slowly. Take $C \approx C_B$ and evaluate κ at $\xi=0$. Let $E=E_Q$ at $\xi=0$ and define the quench level $Q = E_Q/E_0$. Then

$$B \approx B_0 \exp[-(D/v\tau_P)Q^2(1+\kappa^2)^{-1}],$$

$$D = 2RC_B\int_0^\infty (E/E_Q)^2 d\xi = 0.56 \text{ cm}. \tag{A6}$$

D is a characteristic quenching length for our electrodes.[73] Evidently the beam is strongly quenched at the crossing point, $\kappa=0$. The amount of beam quenching depends on choice of quench level Q.

We measure the fraction F of the beam B which *does not* survive passage through the quenching region. Ignoring the slight Zeeman curvature of e_B, take

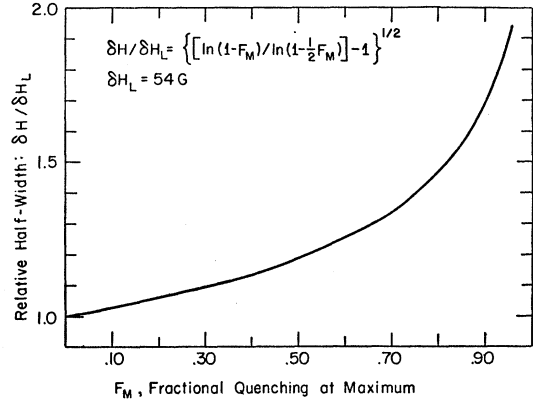$$\kappa \approx \kappa_L[1-(H_0/H_{CB})], \tag{A7}$$

FIG. 8. Full linewidth at half-maximum for the β_B-e_B quenching line shape. The curve is calculated from the Bethe-Lamb theory of the lifetime of the metastable $2S$ state in external fields. F_M is the observed quenching maximum.

where H_0 is the coil central field. Then the quenching fraction

$$F \approx 1-\exp\left\{-(D/v\tau_P)Q^2\left[1+\left(\frac{H_{CB}-H_0}{\delta H_L/2}\right)^2\right]^{-1}\right\}. \tag{A8}$$

This approximate line shape function is symmetric about $H_0 = H_{CB}$. The maximum value F_M at $H_0 = H_{CB}$ depends on the chosen Q. In terms of F_M, the half-width of F is

$$\delta H = \delta H_L\{[\ln(1-F_M)/\ln(1-\tfrac{1}{2}F_M)]-1\}^{1/2}. \tag{A9}$$

This is shown in Fig. 8. For 3000°K H atoms, $v = 6.2 \times 10^5$ cm/sec.[74] For $E_Q = 0.7$ V/cm, $F_M \approx 0.42$ and $\delta H = 62$ G.

Several small effects (Zeeman curvature, matrix element variation, etc.) make F slightly asymmetric about H_{CB}. The observed center of F lies above the true center by about 1 part in 10^4. These effects are discussed in the following Appendix.

APPENDIX II: ASYMMETRY CORRECTIONS

We study the line shape F in detail. Quenching by fields other than the controlled quenching field E is considered. Several corrections which make F asymmetric about H_{CB} are calculated near H_{CB}, to correct the observed line center. The major asymmetry correction is a "natural one," due to magnetic field variation of the Stark matrix element.

Define $r = H_0/H_{CB}$, H_0 the coil central field. For line center measurements, we work in the range $0.96 \leqslant r \leqslant 1.04$. We will approximate the integral in Eq. (A5) for small values of $r-1$.

The quenching field has two sources besides E. There is a motional field E_M experienced by off-axis beam

---

[72] Strictly speaking, the upper limit on the integral should be L/R where $L=20$ cm is the distance from coil center to detector. But $L/R \approx 4$ is a relative infinity with respect to the ξ region where E is appreciable, namely $0 \leqslant \xi \leqslant 0.1$.

[73] See Sec. IIC. This integral was evaluated by the electrolytic tank method.

[74] The beam velocity averaging is carried out by the method in HIII, Ref. 1. Appendix V, using a v^2 distribution (see HIV, Ref. 1, Sec. 79). We need only a simple velocity analysis, since motional Stark quenching is very small in our experiment. We use the average velocity $v = (\pi kT/2m)^{1/2}$.
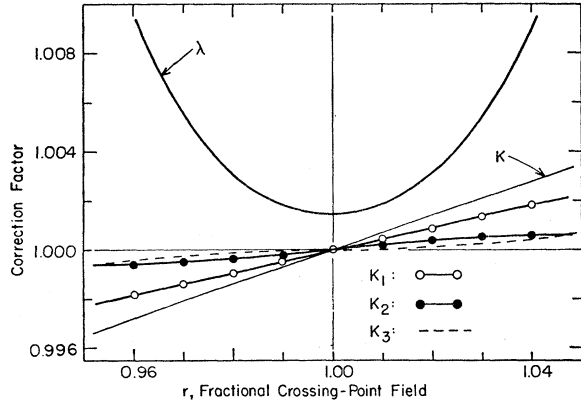
FIG. 9. Line-shape correction factors K and λ. Owing to these factors, the observed line center is shifted by about 1 part in 10^4 above the crossing point at $r=1$.

atoms moving through transverse components of the coil field. For our geometry, we estimate that E_M causes $\approx 4\%$ quenching at $H_0=H_{CB}$. There are also stray fields E' from contact potential differences on the quenching electrodes. From the "beam notch" (Fig. 5), we estimate the E' quenching is equivalent to a spurious E field $\leqslant 0.2$ V/cm.

Taking the square of vectors E, E', and E_M, and averaging over beam trajectories, E^2 in Eq. (A5) becomes: $E^2+2EE_x'+E'^2+E_M^2$, where E_x' is the component of E' along E. We assume E_x' has the same ξ dependence as E. With $E_Q=E(\xi=0)$, and $e=E(\xi)/E_Q$, set $E_x'=(\chi/2)eE_Q$, where χ is independent of ξ. Substituting in Eq. (A6), the E'^2 and E_M^2 integrals are independent of the quench level Q, and may be absorbed in B_0. Then

$$B(Q,r)=B_0(r)\exp\left[-(2R/v\tau_P)Q^2(1+\chi)\right.$$
$$\left.\times\int_0^\infty Ce^2(1+\kappa^2)^{-1}d\xi\right]. \quad (A10)$$

$B_0(r)$ depends on magnetic field; with $Q=0$, it gives the beam notch seen in Fig. 5. But when we take *fractional* quenching (beam flop at level Q divided by total beam), $B_0(r)$ drops out. Thus a normalization to fractional quenching eliminates line asymmetry due to the beam notch.

With x as defined in Sec. IV, the matrix element correction is[75]

$$C=\tfrac{3}{4}(1+\delta), \quad \delta=\tfrac{1}{3}(1+3x)(1+\tfrac{2}{3}x+x^2)^{-1/2}. \quad (A11)$$

$C=1$ at $H=0$, while at the crossing point $(x=x_{CB} \approx 7.75\times10^{-2})$, $C=C_B=1.0496$. C depends on ξ, but varies so slowly over the quenching region that it is

---

[75] See HIII, Ref. 1, Sec. 63. Sec. 46 in BS(57), Ref. 3, gives a detailed discussion.

taken outside the integral. Define: $K_1(r)=C(rx_{CB})/C_B$, and set $C=C_BK_1(r)$ in Eq. (A10).

With v_B given in Sec. IV, $\kappa(x)=4\pi\tau_P v_B(x)$. Expand v_B to order x^2 and take $x=rx_{CB}h(\xi)$, where

$$h(\xi)=1-(144/125)\xi^4, \quad (A12)$$

is the fractional axial coil field[76] in the quenching region. Expand $(1+\kappa^2)^{-1}$ to order ξ^4 and integrate. The result is

$$B(Q,r)=B_0(r)\exp\left[-(D/v\tau_P)Q^2(1+\chi)g(r)K(r)\right],$$
$$g(r)=[1+\kappa_0^2(1-r)^2]^{-1}. \quad (A13)$$

D is given in Eq. (A6). $g(r)$ is resonant at $r=1$.[77] K is a composite correction factor: $K=K_1K_2K_3$. All $K_i=1$ at $r=1$, and increase with increasing r. They raise the observed line center above true center at $r=1$. K_1 has been given above. K_2 is a fs and hfs curvature correction. K_3 is due to the finite size of the quenching region.[78] The K_i are graphed in Fig. 9. Note that the natural correction K_1 is largest. To good approximation

$$K(r)=1+s(r-1), \quad s=6.947\times10^{-2}. \quad (A14)$$

The beam flop is $\Delta B(Q,r)=B(0,r)-B(Q,r)$. At constant r, ΔB versus Q^2 gives a quenching curve as in Fig. 6. For the total beam B_T, we choose $Q=Q_P$ so $\Delta B(Q_P,r)$ lies just above the "knee" of the quench plateau. Measuring ΔB at Q_P, $\sqrt{2}Q_P$, and $2Q_P$, we take the least-squares linear extrapolation

$$B_T(Q_P,r)=\Delta B(Q_P,r)-\tfrac{1}{2}[\Delta B(2Q_P,r)-\Delta B(\sqrt{2}Q_P,r)]$$
$$\approx[1-O(10^{-3})]B_0(r). \quad (A15)$$

The quenching exponent involving Q_P is chosen to be $\geqslant 7$. Because it depends on K, B_T increases slightly with r. This causes a slight asymmetry about $r=1$.

As remarked in Sec. IIIB, there is an α-f contribution to the β_B-e_B quenching. This is small, since the α-f separation is about 2200 Mc near the crossing point, $r\approx 1$. It introduces a slight line asymmetry. Taking this into account to order Q^2 in $\Delta B(Q,r)$, we can write the fractional quenching $\Delta B(Q,r)/B_T$ as

$$F(Q,r)=\lambda(r)\{1-\exp[-(D/v\tau_P)Q^2(1+\chi)g(r)K(r)]\}. \quad (A16)$$

$\lambda(r)$ includes the B_T correction as well as the α-f contribution. It lowers the observed center by about 10 ppm. It is graphed in Fig. 9. Note that since χ is independent of magnetic field, it causes no asymmetry. With F reaching its maximum value F_M at $r\approx 1$, we take (to good approximation)

$$-(D/v\tau_P)Q^2(1+\chi)=\ln(1-F_M). \quad (A17)$$

---

[76] This is the expansion for a perfect Helmholtz coil. See J. Reitz and F. Milford, *Foundations of Electromagnetic Theory* (Addison-Wesley Publishing Company, Inc., 1960), 1st ed., p. 157.

[77] $\kappa_0=\kappa_L(1-\zeta)$ is corrected by ζ due to fs and hfs curvature.

[78] $K_3(r)=1+2A\kappa_0^2r(r-1)g(r)$, for small $r-1$. $A \leqslant 26$ ppm is given in Sec. IIC. Owing to K_3 alone, the observed center occurs at $r=1+A$.